Molecular Biotechnology (2023) 65:612–623
https://doi.org/10.1007/s12033-022-00559-0

ORIGINAL PAPER

Knockdown of Krüppel-Like Factor 9 Inhibits Aberrant Retinal Angiogenesis and Mitigates Proliferative Diabetic Retinopathy

Ning Han[1] · Lihong Zhang[2] · Mi Guo[3] · Li Yu[1]

Received: 12 April 2022 / Accepted: 5 September 2022 / Published online: 15 September 2022

Abstract

Advanced proliferative diabetic retinopathy (PDR) characterized by aberrant retinal angiogenesis is a leading cause of retinal detachment and blindness. Krüppel-like factor 9 (KLF9), a member of the zinc-finger family of transcription factors, participates in the development of diabetic nephropathy and the promotion of angiogenesis of human umbilical vein endothelial cells. Therefore, we speculate that KLF9 may exert a crucial role in PDR. The current study revealed that KLF9 was highly expressed in the high glucose (HG)-treated human retinal microvascular endothelial cells (HRMECs) and the retinas of oxygen-induced retinopathy (OIR) rats. Knockdown of KLF9 inhibited the proliferation, migratory capability, invasiveness and tube formation of HG-treated HRMECs. Besides, knockdown of KLF9 decreased the expression of yes-associated protein 1 (YAP1) in HG-treated HRMECs. Dual-luciferase reporter assays confirmed that KLF9 transcriptionally upregulated YAP1 expression. Overexpression of YAP1 reversed the KLF9 silencing-induced repression of HRMEC proliferation and tube formation. Further in vivo evidence demonstrated that knockdown of KLF9 reduced the expression of Ki67, CD31 and vascular endothelial growth factor A (VEGFA) in the retinas of OIR rats. Collectively, KLF9 silencing might mitigate the progression of PDR by inhibiting angiogenesis via blocking YAP1 transcription.

Keywords Angiogenesis · Krüppel-like factor 9 · Proliferative diabetic retinopathy · Yes-associated protein 1

Introduction

Diabetic retinopathy (DR) is the most frequent microvascular complication of diabetes and its global prevalence has increased in the past 10 years [1]. DR is divided into the early-stage non-proliferative DR (NPDR) and the end-stage proliferative DR (PDR) [2]. PDR is mainly characterized by ischemia-induced neovascularization, which results in retinal detachment and blindness [3]. In PDR, hyperglycemia alters the retinal microenvironment and causes microvascular endothelial cell dysfunction and vascular endothelial growth factor (VEGF) upregulation, ultimately leading to neovascularization [4]. Currently, laser photocoagulation, vitrectomy and anti-VEGF drugs are available in the treatment of PDR. However, accumulating clinical studies report the undesirable side effects of these therapies [5, 6]. Therefore, a deeper exploration of the pathogenesis of PDR is necessary, which may contribute to developing more effective treatments.

Krüppel-like factor 9 (KLF9), also called basic transcription element-binding protein 1 (BTEB1), is a member of the zinc-finger family of transcription factors and participates in a series of physiopathological processes, such as cell proliferation, apoptosis, and invasion [7, 8]. KLF9 has been known to exert a key role in diabetes and diabetic complications. KLF9 was highly expressed in the serum of patients with diabetic nephropathy, and its overexpression aggravated high glucose (HG)-induced podocyte injury [9]. Hepatic knockdown of KLF9 in diabetic mice mitigated hyperglycemia induced by chronic dexamethasone treatment [10]. KLF9 deficiency protected human neuroblastoma cells SH-SY5Y from HG-aggregated bupivacaine neurotoxicity [11]. Thus, downregulation of KLF9 might protect against hyperglycemia-induced cellular injury. Ma et al. [12] found

✉ Li Yu
yuli_oculist@jlu.edu.cn

1 Department of Ophthalmology, The Second Hospital of Jilin University, Nanguan District, No.218, Ziqiang Street, Changchun, Jilin, China

2 Department of Ophthalmology, Songyuan Derun Tongxin Hospital, Songyuan, Jilin, China

3 Department of Ophthalmology, Baotou Eye Hospital, Baotou, Inner Mongolia Autonomous Region, China

that upregulation of KLF9 accelerated the vascularization of human umbilical vein endothelial cells (HUVECs) via directly binding to the VEGFA promoter [12]. Based on the aforementioned findings, we speculated that KLF9 might be involved in the progression of PDR by regulating neovascularization.

Yes-associated protein 1 (YAP1), as a transcriptional coactivator, is a crucial effector of the conserved Hippo signaling pathway that controls carcinogenesis, regeneration and metabolism [13]. Sustained HG environment can activate the Hippo pathway and increase the expression levels of YAP1, thereby facilitating cell proliferation and invasion [14]. Numerous studies have demonstrated that highly expressed YAP1 contributes to the development of diabetes-related diseases, including diabetic nephropathy, diabetic cardiomyopathy, and diabetic retinopathy [15–18]. Wang et al. [19] showed that downregulation of YAP1 by folic acid attenuated HG-induced retinal vascular endothelial injury [19]. Evidence suggested that YAP1 upregulated VEGFA expression via induction of hypoxia inducible factor-1α (HIF-1α) in retinal tissues of diabetic mice [17]. We previously found that silencing of YAP1 repressed the proliferation, migration and tube formation in HG-induced human retinal microvascular endothelial cells (HRMECs) [18]. These findings suggested that YAP1 was a potential regulator in the progression of PDR.

Bioinformatics analysis shows that there are potential binding sites between KLF9 and the promoter region of YAP1. However, whether YAP1 was required for KLF9-mediated PDR progression remains unknown. To study the role of KLF9 in pathological neovascularization, we established a rat model of oxygen-induced retinopathy (OIR) according to the previous description [20]. Similar to human PDR, neovascularization occurs in the retina of OIR rats, in which proliferative retinopathy can develop reliably over 17 days [21]. It is well-known that HG can induce angiogenesis and endothelial cell dysfunction in vitro [22–24]. Thus, HG-treated HRMECs were used as an in vitro model to further study the function of KLF9 in hyperglycemia-associated cellular injury and its potential regulatory mechanism involving in YAP1.

Results

KLF9 Is Highly Expressed in HG-Induced HRMECs

To explore the role of KLF9 in PDR, we used HG-treated HRMECs to mimic PDR-induced cellular injury in vitro. The expression of KLF9 in HRMECs exposed to HG was detected using real time-polymerase chain reaction (RT-PCR) and western blotting assays. A significant upregulation of KLF9 mRNA and protein expression was observed in HRMECs treated with HG, compared to that in HRMECs treated with normal glucose (NG) or mannitol (Mann) (Fig. 1A and B $p < 0.05$). Immunofluorescence analysis confirmed upregulated KLF9 expression in HG-induced HRMECs (Fig. 1C).

Knockdown of KLF9 Represses Proliferation and Tube Formation of HG-Induced HRMECs

Two small interfering RNAs were designed to silence KLF9 expression and reduce the off-target effect (Fig. 2A and B). The expression of KLF9 was effectively downregulated in NG-treated HRMECs ($p < 0.05$). To assess the effect of KLF9 on cellular injury induced by HG, siKLF9s or its negative control (siNC) were transfected into HRMECs and then treated with HG. As shown in Fig. 2C and D, knockdown of KLF9 efficiently downregulated KLF9 mRNA and protein expression in HG-induced HRMECs ($p < 0.05$). By performing cell counting kit-8 (CCK-8) assays, we determined that knockdown of KLF9 significantly inhibited HG-induced cell proliferation (Fig. 2E, $p < 0.05$). Results of immunofluorescence staining showed that knockdown of KLF9 downregulated Ki67 (a marker of cell proliferation) expression in HG-induced HRMECs (Fig. 2F). Also, knockdown of KLF9 inhibited HG-induced tube formation (Fig. 2G, $p < 0.05$).

Knockdown of KLF9 Inhibits the Migration and Invasion of HG-Induced HRMECs

Wound healing and Transwell assays were used to evaluate the effect of KLF9 on migratory and invasive abilities of HG-induced HRMECs. Results showed that HG promoted wound closure and invasion of HRMECs (Fig. 3A and B, $p < 0.05$). Knockdown of KLF9 reduced wound closure rate and invaded cell number in HG-induced HRMECs (Fig. 3A and B, $p < 0.05$). Besides, protein levels of active matrix metalloproteinase (MMP) 2 and MMP9 in HG-induced HRMECs were reduced after KLF9 silencing (Fig. 3C, $p < 0.05$).

KLF9 Transcriptionally Upregulates YAP1

We next sought to investigate the underlying mechanism of KLF9 in HG-induced HRMECs. Human Transcription Factor Database (TFDB) showed several potential binding sites between the sequence of KLF9 and the promoter region of YAP1. We detected the expression of YAP1 in HG-induced HRMECs by RT-PCR and western blotting assays. Results revealed that the expression of YAP1 was significantly upregulated in HG-treated HRMECs, compared to that in NG-treated HRMECs. KLF9 knockdown inhibited HG-induced YAP1 mRNA and protein upregulation in HRMECs (Fig. 4A and B, $p < 0.05$). Subsequent

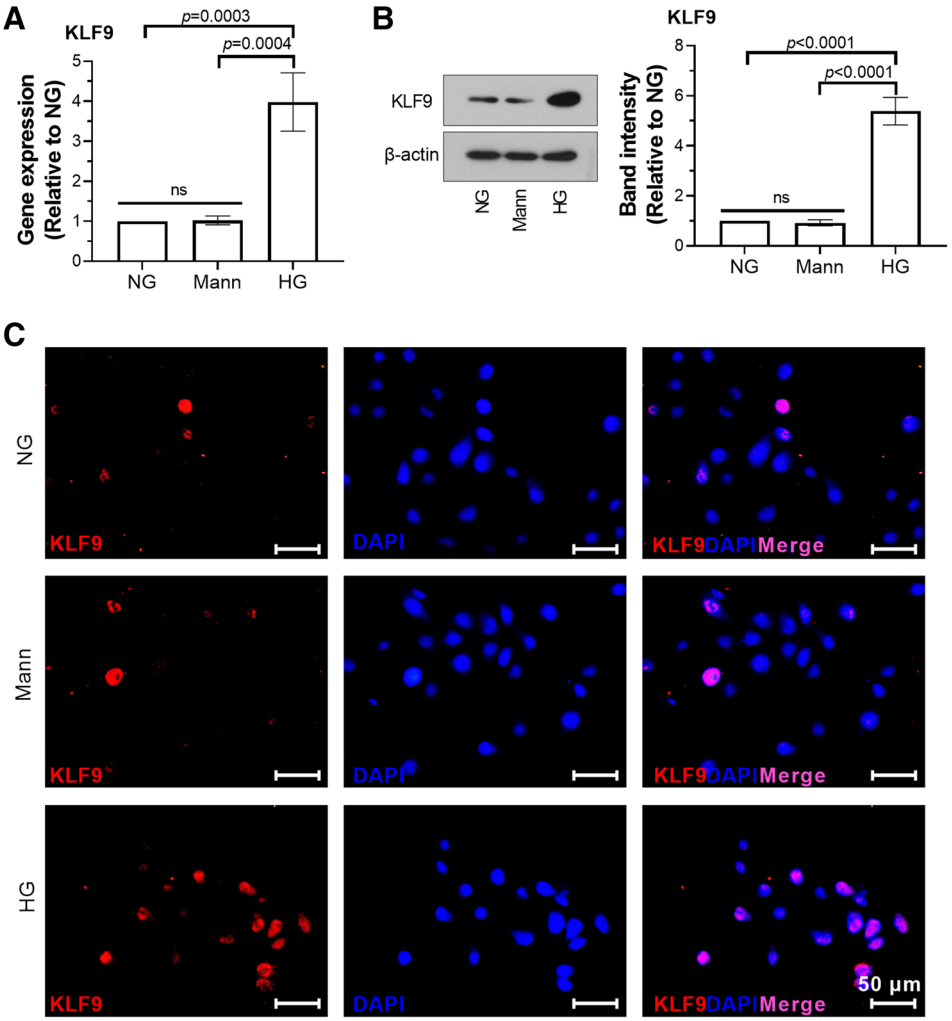

Fig. 1 KLF9 is highly expressed in HG-treated HRMECs. **A** Relative mRNA expression of KLF9 in HRMECs was measured by RT-PCR. **B** Relative protein expression of KLF9 in HRMECs was determined by western blotting. **C** Immunofluorescence analysis of KLF9 in HRMECs was performed. Bars = 50 μm. RT-PCR: real time-polymerase chain reaction; KLF9: krüppel-like factor 9; HRMECs: human retinal microvascular endothelial cells; NG: normal glucose; HG: high glucose; Mann: osmotic control. $n = 3$ replications per group

dual-luciferase reporter assays verified the regulation of KLF9 on YAP1 transcription. We found that KLF9 overexpression significantly enhanced the luciferase activity of YAP1 in HEK293T cells (Fig. 4C, $p < 0.05$). In addition, deletion of YAP1 promoter region −2000/−1200 bp caused a great decrease in YAP1 luciferase activity. There is no obvious difference in YAP1 luciferase activity after deleting fragment −1200/−400 bp. These data indicated that KLF9 transcriptionally activated YAP1 by binding to the putative site within the YAP1 promoter region −2000/−1200 bp.

YAP1 Is Involved in KLF9-Mediated HRMEC Proliferation and Tube Formation

To unveil whether YAP1 was involved in KLF9-mediated cell proliferation and tube formation, siKLF9 was co-transfected with exYAP1 or vector into HRMECs. We found that the KLF9 silencing-induced YAP1 downregulation in HG HRMECs was reversed by YAP1-overexpressing plasmid (exYAP1) (Fig. 5A, $p < 0.05$). Additional functional experiments suggested that YAP1 overexpression partially reversed KLF9 silencing-induced proliferation and tube formation inhibition in HG HRMECs (Fig. 5B and C, $p < 0.05$).

Knockdown of KLF9 Inhibits Retinal Angiogenesis and Mitigates PDR in OIR Rats

We further determined the effect of KLF9 in OIR rats. Compared with the sham group, the mRNA expression of KLF9 was upregulated in the retinas of OIR rats. Lentivirus-mediated RNAi knockdown of KLF9 was confirmed in OIR rats after intravitreal injection with lentivirus carrying short hairpin RNA (shRNA) targeting KLF9 (LV-shKLF9) (Fig. 6A, $p < 0.05$). H&E staining revealed that knockdown of KLF9 decreased retinal thickness and blood vessel profiles in OIR rats (Fig. 6B). Reduced Ki67 expression was observed in the retinas of OIR rats after KLF9 knockdown (Fig. 6B). Besides, knockdown of KLF9 suppressed VEGF expression in the retinas of OIR rats (Fig. 6C, $p < 0.05$). Representative immunofluorescence staining for CD31 showed

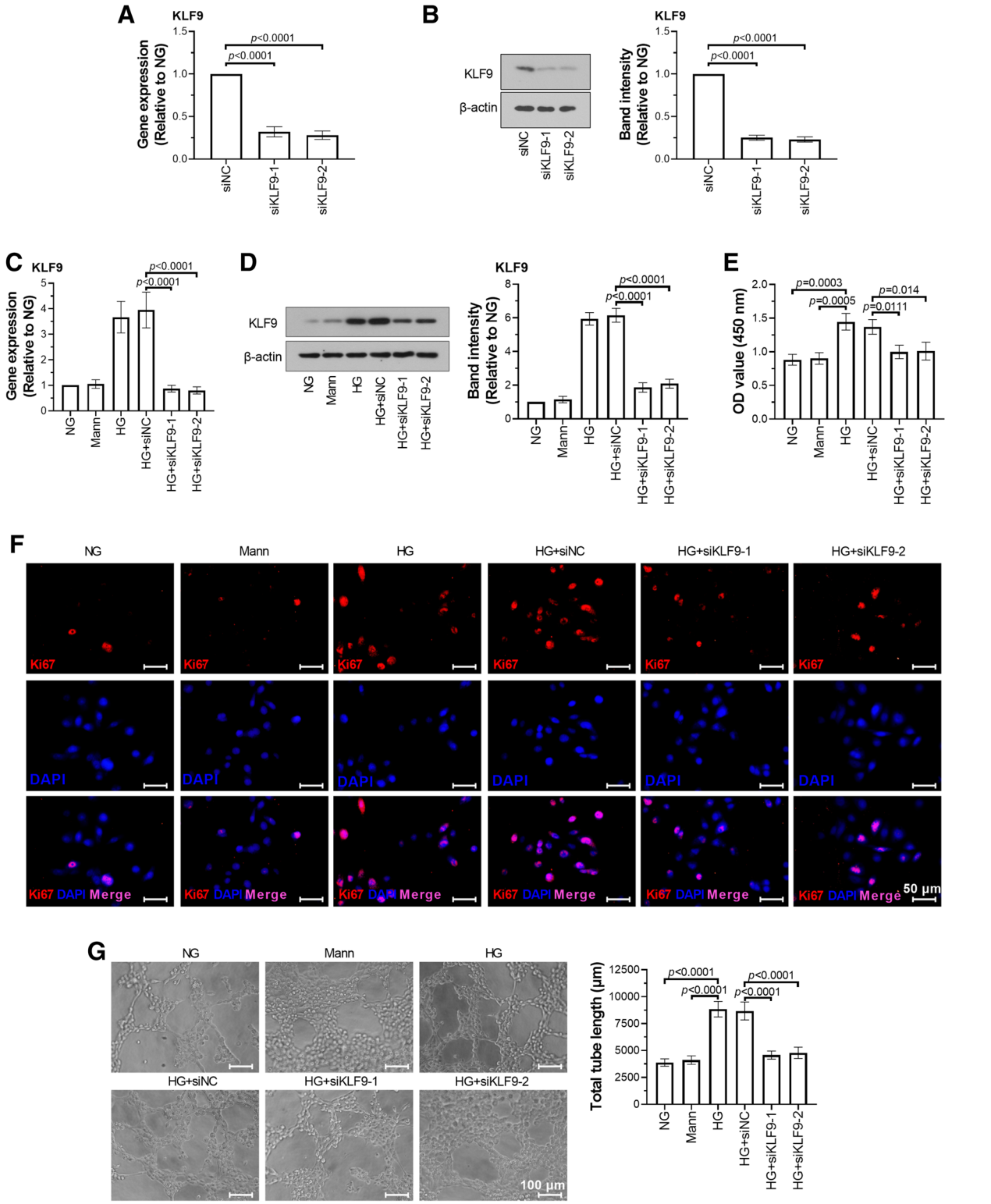

that knockdown of KLF9 reduced the new vessel formation in OIR rats (Fig. 6D).

Discussion

Despite decades of effort, effective therapies for PDR angiogenesis remain to be developed due to its elusive mechanism [25]. The present study sought to investigate

◂**Fig. 2** Knockdown of KLF9 represses proliferation and tube formation of HG-induced HRMECs. Relative **A** mRNA and **B** protein expression of KLF9 in NG-treated HRMECs was measured to determine the interference efficient. **C** Relative mRNA expression of KLF9 in HRMECs was measured by RT-PCR. **D** Relative protein expression of KLF9 in HRMECs was determined by western blotting. **E** CCK-8 assay was performed to assess HRMEC viability. **F** Immunofluorescence analysis of Ki67 (proliferation index marker) in HRMECs. Bars = 50 μm. **G** Tube formation assay was used to evaluate vascularization of HRMECs. Bars = 100 μm. NG: normal glucose; HG: high glucose; Mann: osmotic control; siKLF9: small interfering RNA targeting KLF9; siNC: negative control; RT-PCR: real time-polymerase chain reaction; KLF9: krüppel-like factor 9; CCK-8: cell counting kit-8; HRMECs: human retinal microvascular endothelial cells. $n = 3$ replications per group

whether KLF9 participated in PDR angiogenesis and elucidate its potential mechanisms of action. We found that KLF9 was highly expressed in HG-induced HRMECs and the retinas of OIR rats. Knockdown of KLF9 inhibited the proliferation, migration, invasion and tube formation of HG-treated HRMECs, as well as reduced angiogenesis in the retinas of OIR rats. Dual-luciferase reporter assays confirmed that KLF9 transcriptionally upregulated YAP1 expression. Re-expression of YAP1 reversed KLF9 silencing-induced inhibition of proliferation and tube formation in HRMECs upon HG condition. Collectively, KLF9 might contribute to PDR angiogenesis via directly activating YAP1 transcription.

In this study, a rat model of OIR was used to investigate the pathophysiology of ischemic retinopathy. Unlike chronic hyperoxia, the model is established through alternating hyperoxia/hypoxia exposure. Exposure to cycling oxygen causes capillary non-perfusion in the periphery of the rat retina. After backing to room air, pathologic neovascularization occurs at the border between vascular and avascular regions in the midperiphery of retina [26]. VEGF is a major inducer driving angiogenesis. Upon binding to its receptor, VEGF increases the proliferation and migration of endothelial cells, thereby inducing angiogenesis [27]. Under hypoxic condition, cellular HIF-1α protein is stabilized, subsequently translocates into the nucleus and forms a complex with HIF-1β. The heterodimeric HIF-1α/HIF-1β transcription factor complex recognizes the hypoxia-responsive elements and triggers the transcription of target genes, such as VEGF [28]. A previous study by our group has reported that miR-203a-3p overexpression inhibits retinal neovascularization in OIR rats by downregulation of VEGFA and HIF-1α [29]. It has been identified that KLF9 upregulation assists in the production of myocardial VEGF and the development of malignant phenotypes of diabetic rats [30]. In the current study, we observed that knockdown of KFL9 inhibited the tube formation of HRMECs upon HG condition. KLF9 silencing decreased vascularization and the level of VEGF in retinas of OIR rats.

Angiogenesis is regulated by the activation, proliferation and invasion of endothelial cells, which is associated with the degradation of basement membrane and the remodeling of extracellular matrix [31, 32]. MMPs, particularly MMP2 and MMP9, have been implicated in this process [33]. It has been identified that KLF9 enhances the tube formation of HUVECs via upregulating VEGFA expression (12). In the present study, a reduction of MMP2 and MMP9 in HG-treated HRMECs was observed after KLF9 silencing. This finding was in contrast to a previous study in tumor cells [34], which might be explained by different downstream target genes of KLF9 in the tumor. Knocking KLF9 down also inhibited cell proliferation in the HG-treated HRMECs and the retinas of OIR rats, thus supporting the role of KLF9 in neovascularization of PDR.

YAP1 has been well characterized to modulate the angiogenesis of retinal microvascular endothelial cells [35]. A previous study suggested that Sirtuin 1 (SIRT1) overexpression repressed the angiogenesis in the retinas of diabetic mice, and inhibited the proliferation and tube formation in HG-treated mouse RMECs via downregulation of YAP/HIF1α/VEGFA [17]. Deficiency of YAP inhibited choroidal neovascularization by reducing endothelial cell proliferation [36]. We previously confirmed that YAP1 was a crucial regulator of aberrant retinal angiogenesis in DR and its downregulation was effective to hinder pathologic angiogenesis in DR mice and HG-induced mouse RMECs [18]. Here, we further identified that YAP1 is the target gene of KLF9, implying that YAP1 might be involved in KLF9's function in PDR. Subsequent rescue experiments demonstrated that reintroduction of YAP1 partially reversed KLF9 silencing-induced repression of HRMEC proliferation and tube formation. Therefore, the function of KLF9 in PDR may be achieved through the following ways: (1) inducing upregulation of VEGF and MMP-2/9 via stabilizing HIF-1α in hypoxic HRMECs, and (2) regulating cell proliferation, migration, invasion and angiogenesis by upregulating YAP1/VEGF.

Although DR has long been defined as vascular disease, increasing evidence has illustrated that the dysfunction of retinal neuronal cells, such as retinal ganglion cells (RGCs), is involved in DR-related visual loss [37, 38]. Two previous studies showed that the expression of KLF9 is detectable in RGCs, and its overexpression inhibits RGC axon regeneration [39, 40], implying a role of KLF9 in optic nerve crush. We here demonstrated that KLF9 contributed to DR progress with a focus on RMECs. However, to fully understand the role of KLF9 in DR development, there is also a need to investigate its function across different cell types of the retina, such as RGCs.

In summary, the current study uncovers that inhibition of KLF9 likely attenuates the progression of PDR. In detail, knockdown of KLF9 inhibited the proliferation, migration, invasion and angiogenesis by transcriptionally downregulating

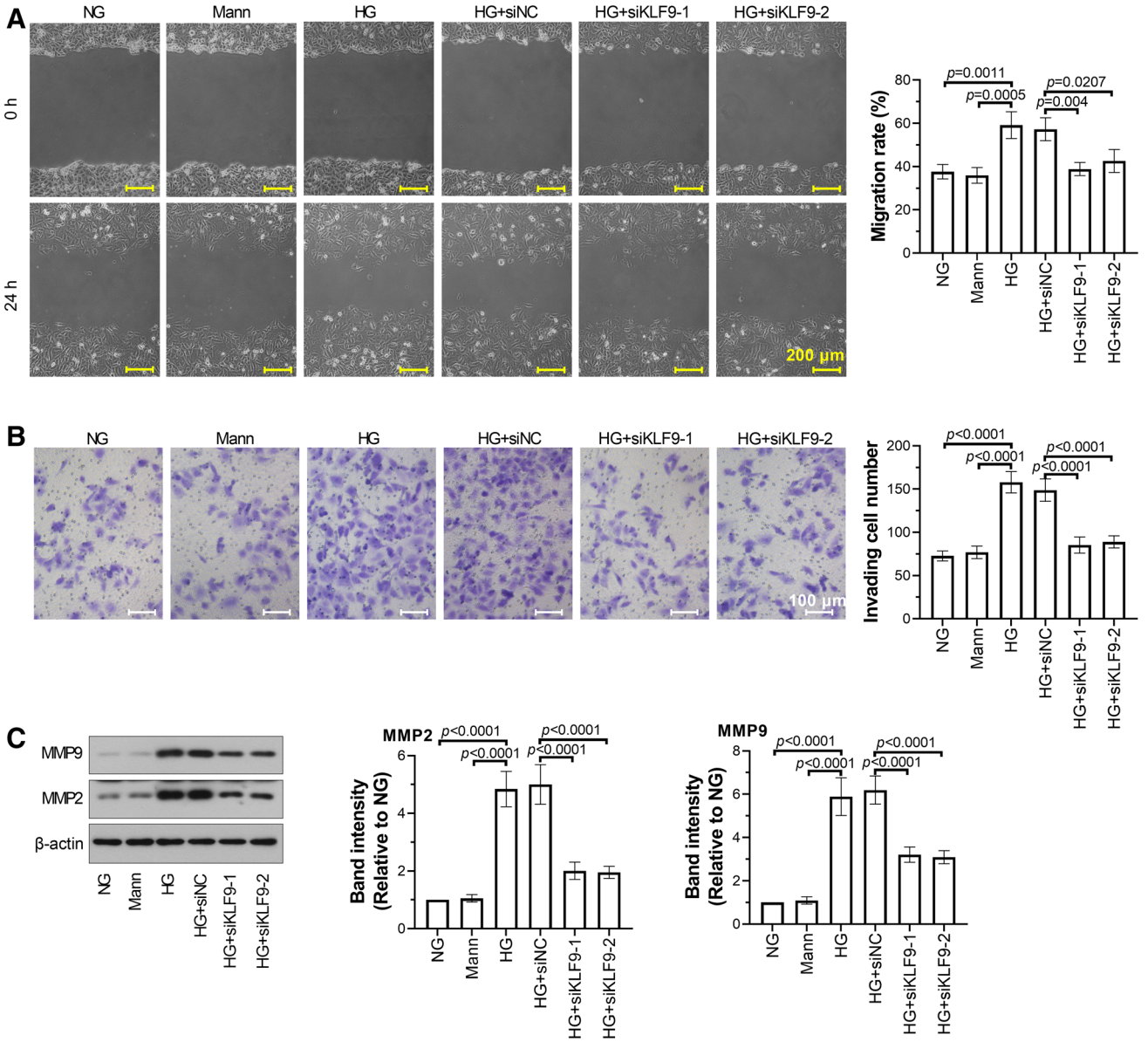

Fig. 3 Knockdown of KLF9 inhibits the migration and invasion of HG-induced HRMECs. **A** Images were photographed at 0 h and 24 h after scratching. Bars = 200 μm. The percentage of migration distance at 24 h was quantified. **B** Cells were seeded on matrigels and allowed to invade for 24 h at 37 °C. The images were photographed (Bars = 100 μm) and the invading cell number was quantified. **C** Relative protein expression of MMP2 and MMP9 in HRMECs was determined by western blotting. KLF9: krüppel-like factor 9; NG: normal glucose; HG: high glucose; Mann: osmotic control; siKLF9: small interfering RNA targeting KLF9; siNC: negative control; MMP2/9: matrix metalloproteinase 2/9; HRMECs: human retinal microvascular endothelial cells. $n = 3$ replications per group

YAP1 in HG-stimulated HRMECs and the retina of OIR rats. Therefore, our study indicates that KLF9 may be a novel factor in the pathogenesis of PDR, suggesting a potential therapeutic target for PDR.

Materials and Methods

Cell Culture

HRMECs (Procell, China) were grown at 37 °C with 5% CO_2 in endothelial cell medium (Icellbioscience, China) containing 5% fetal bovine serum (FBS; SH30084.03,

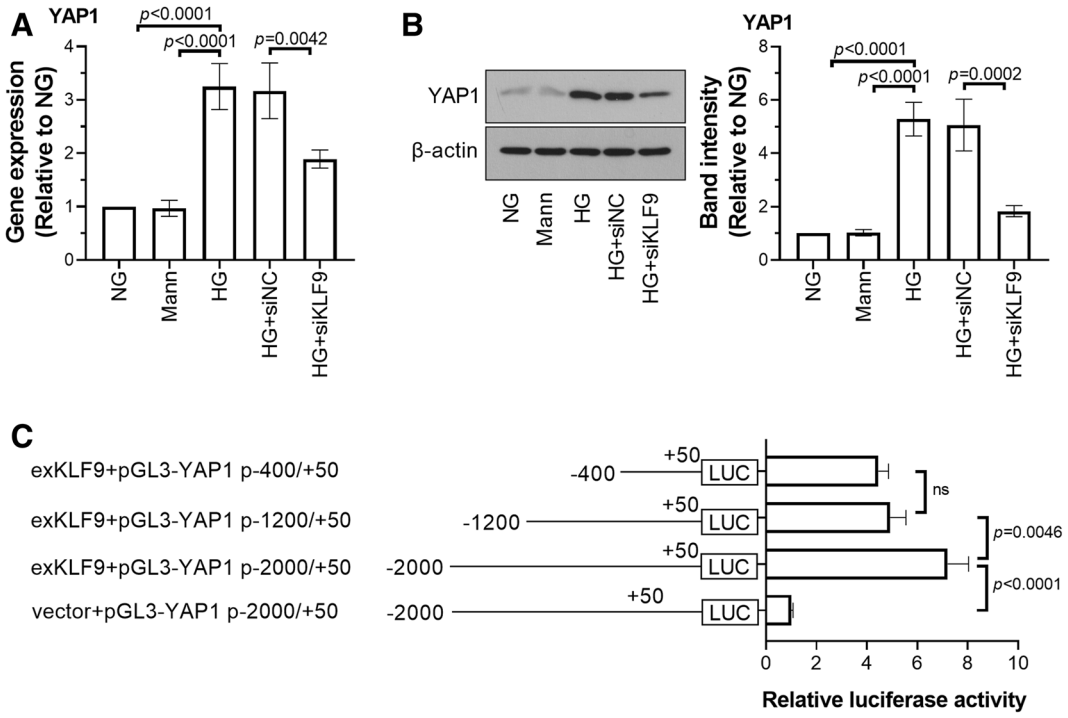

Fig. 4 KLF9 transcriptionally upregulates YAP1. **A** Relative mRNA expression of YAP1 in HRMECs was measured by RT-PCR. **B** Relative protein expression of YAP1 in HRMECs was determined by western blotting. **C** Dual-luciferase reporter assay was performed to determine the effects of KLF9 on YAP1 luciferase activity in HEK293T cells. NG: normal glucose; HG: high glucose; Mann: osmotic control; siKLF9: small interfering RNA targeting KLF9; siNC: negative control; RT-PCR: real time-polymerase chain reaction; HRMECs: human retinal microvascular endothelial cells; KLF9: krüppel-like factor 9; YAP1: yes-associated protein 1. $n=3$ replications per group

Hyclone, USA) and 1% endothelial cell growth supplement (Icellbioscience) according to a previous study [41]. To determine the role of KLF9 in PDR in vitro, cells were cultured in endothelial cell medium supplemented with 30 mM D-glucose (B21882, Yuanye, China; regarded as HG group), 5.5 mM D-glucose (control; regarded as NG group), or 24.5 mM mannitol plus 5.5 mM D-glucose (osmotic control; regarded as Mann group; M108831, Aladdin, China) for 48 h as previously described [42].

Cell Transfection

HRMECs were seeded in 6-well plates at a density of 4×10^5 and incubated at 37 °C with 5% CO_2 for 24 h. siKLF9 or siNC (75 pmol, JTS scientific, China) were transfected into cells using Lipofectamine 3000 (L3000015, Invitrogen, USA). *Homo* exYAP1 (1.25 μg; Sino Biological, China) was co-transfected with siKLF9 (37.5 pmol) into cells using Lipofectamine 3000. HG treatment was performed 24 h after cell transfection.

Migration Assay

The migratory ability of HRMECs was evaluated with the wound healing assay. HRMECs were grown to confluence and incubated with mitomycin C (1 μg/Ml; M0503, Sigma, USA) for 1 h. Subsequently, the cell monolayer was scratched with a 200 μl pipette tip to create a wound. After being washed using a serum-free medium, the cells were incubated in a fresh medium at 37 °C with 5% CO_2 for 24 h. Images were photographed at 0 and 24 h post-wounding under an inverted microscope (at × 100 magnification; IX53, Olympus, Japan). The migration distance at 24 h was calculated by subtracting the wound scratch distance at 24 h from that at 0 h.

Transwell Assay

Transwell assay was used to assess cell invasion. Cells (4×10^4 cells/well) were resuspended in a 200 μl serum-free medium and inoculated into the upper chamber of the Transwell with an 8.0 μm pore polycarbonate membrane insert (3422, Corning, SA) in a 24-well plate.

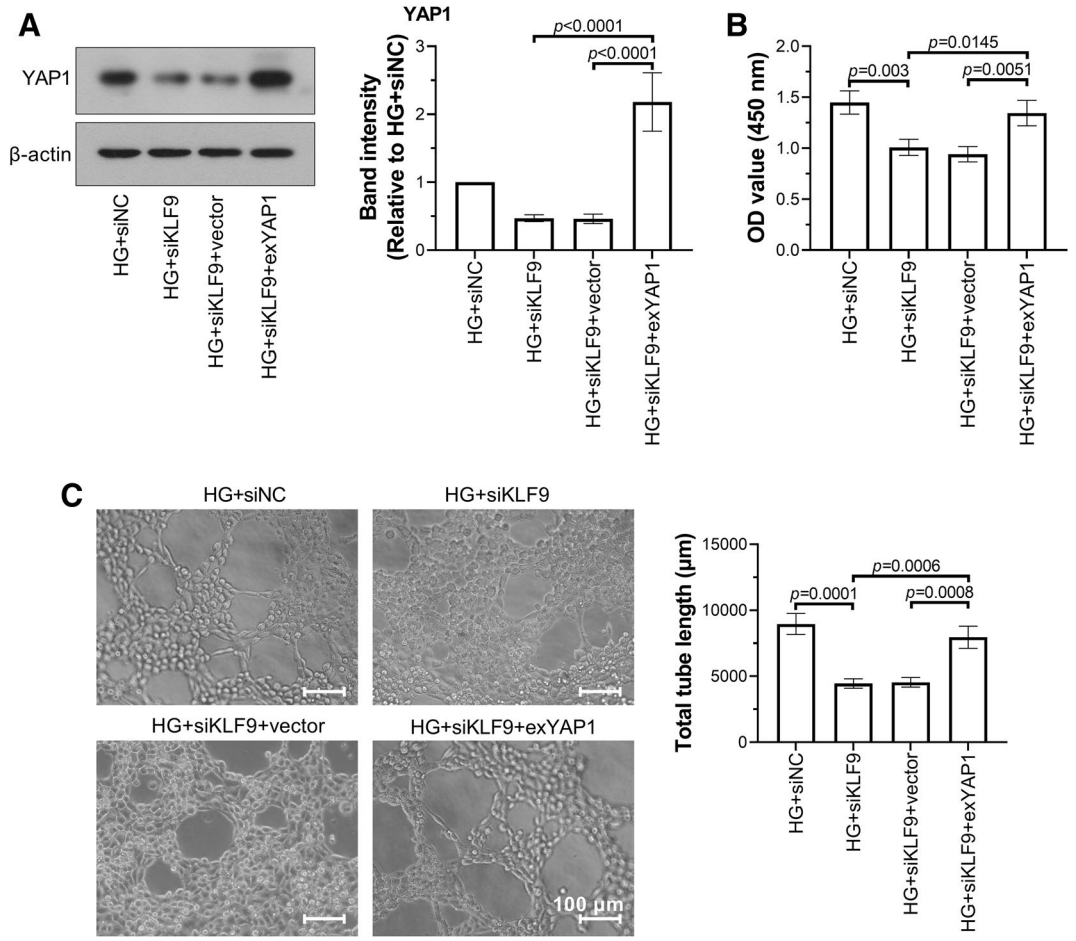

Fig. 5 YAP1 is involved in KLF9-mediated HRMEC proliferation and tube formation. **A** Relative protein expression of YAP1 in HG-induced HRMECs was determined by western blotting. **B** CCK-8 assay was performed to assess HG-induced HRMEC proliferation. **C** Tube formation assay was used to evaluate vascularization in HRMECs co-transfected with siKLF9 and exYAP1 under HG condition. Bars = 100 μm. YAP1: yes-associated protein 1; KLF9: krüppel-like factor 9; CCK-8: cell counting kit-8; siKLF9: small interfering RNA targeting KLF9; exYAP1: YAP1 overexpression plasmid; HG: high glucose; siNC: negative control; HRMECs: human retinal microvascular endothelial cells. $n = 3$ replications per group

Subsequently, 800 μl of the medium containing 10% FBS was added into the lower chamber. After 24 h, the filter membranes were fixed with 4% paraformaldehyde (C104188, Aladdin) for 25 min and stained with 0.4% crystal violet (0528, Amresco, USA) for 5 min. The cells that failed to invade through the membranes were wiped off with cotton balls. The stained cells were observed under inverted microscopy (at × 200 magnification; IX53, Olympus). Five random fields were selected from each well and the mean number of the cells invaded through the filter membranes was calculated. The invading cell number was calculated by the mean of three wells for each sample.

Tube Formation Assay

A total of 50 μl matrigel (354,234, Corning) was added to a 96-well plate and then hardened at 37 °C for 2 h. HRMEC suspensions (1×10^4 cells/well) were plated onto the surface of matrigel, incubated for tube formation at 37 °C for 16 h and photographed using phase-contrast microscopy (at × 200 magnification) (IX53, Olympus). Total tube length was quantified to assess tube formation ability by Image-pro plus 6.0 software (Media cybernetics, Inc.)

Dual-Luciferase Reporter Assay

HEK293T cells were seeded in 12-well plates in complete Dulbecco's modified Eagle's medium (DMEM; Sino Biological) containing 10% FBS and incubated at 37 °C with

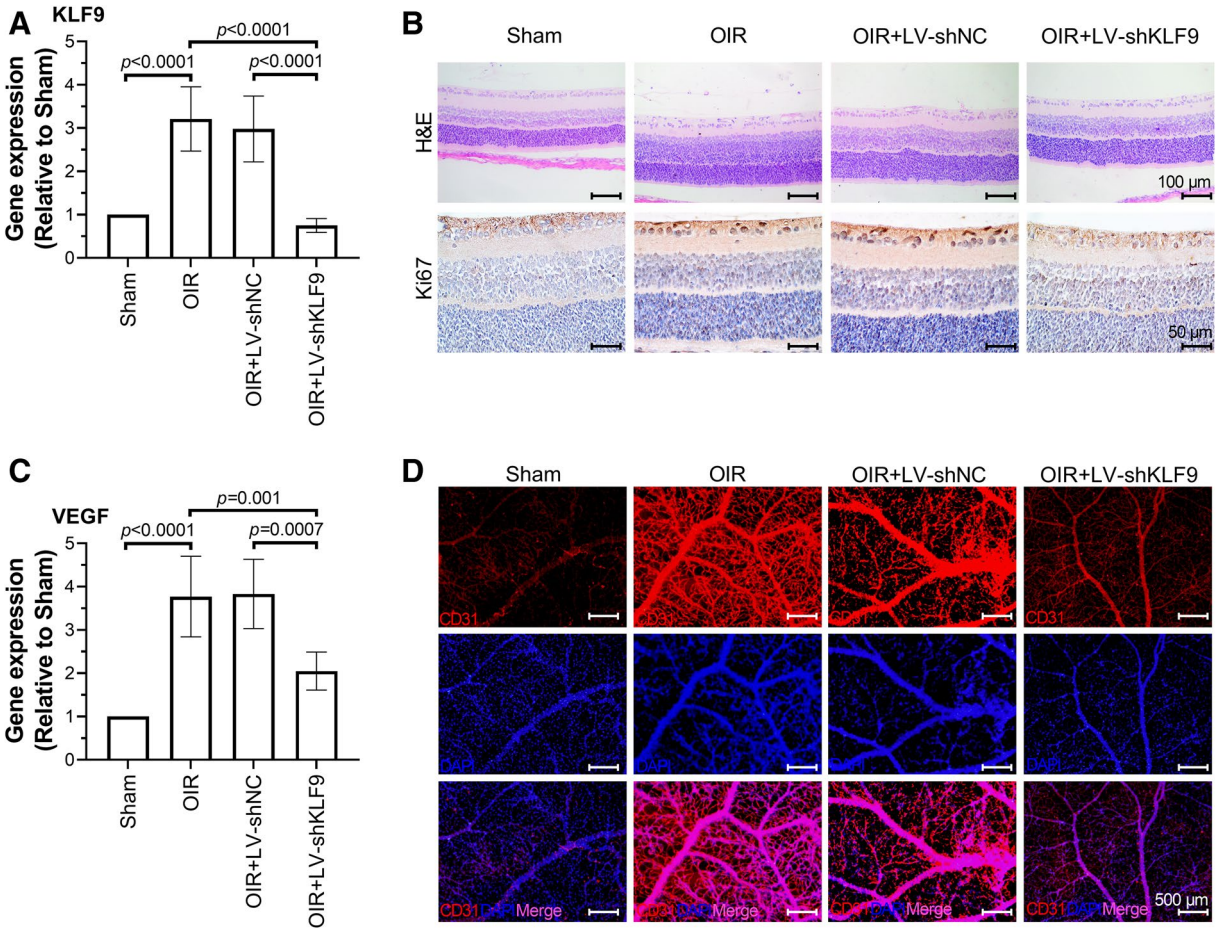

Fig. 6 Knockdown of KLF9 inhibits retinal angiogenesis and mitigates PDR in OIR rats. **A** Relative mRNA expression of KLF9 in the retinas of rats was measured by RT-PCR. **B** H&E staining (Bars = 100 μm) and Ki67-immunohistochemical analysis (Bars = 50 μm) in the retinas of rats. **C** Relative mRNA expression of VEGF in the retinas of rats was measured by RT-PCR. **D** Immunofluorescence analysis of CD31 (a biomarker of endothelial cells) in the retinas of rats. Bars = 500 μm. KLF9: krüppel-like factor 9; LV-shKLF9: KLF9 RNAi lentivirus; LV-shNC: control RNAi lentivirus; VEGF: vascular endothelial growth factor. $n = 6$ replications per group

5% CO2 for 24 h. Next, *homo* YAP1 promoter fragments, including −2000 to + 50, −1200 to + 50 and −400 to + 50 bp, were cloned into the dual luciferase expression vector pGL3-basic. A total of 3 μg plasmids, including 1 μg recombinant pGL3 plasmid or pGL3-basic (empty vector control), 1 μg *homo* KLF9-overexpressing plasmid (exKLF9; Sino Biological) and 1 μg pRL-TK (Promega, USA), were transfected into 293 T cells. After transfection for 24 h, the relative luciferase activity was detected using the Dual-Luciferase Reporter assay kit (E1910, Promega) and normalized to *Renilla* luciferase activity.

Western Blotting

HRMECs were lysed in RIPA lysis buffer (R0010, Solarbio, China). The protein samples were separated by 10–12% SDS-PAGE, followed by transfer to PVDF membranes (IPVH00010, Millipore, USA). After blocking with 5% skim milk, the membranes were incubated with the following primary antibodies at 4 °C overnight: anti-KLF9 (A7196, Abclonal, Wuhan, China; 1:2000), anti-MMP2 (10373-2-AP, Proteintech, Wuhan, China; 1:500), anti-MMP9 (10375-2-AP, Proteintech; 1:1000), anti-YAP1 (A1002, Abclonal; 1:500) and anti-β-actin (sc-47778, Santa Cruz, Dallas, Texas, USA; 1:1000). After washing with TBST, the membranes were then incubated with corresponding secondary antibodies (SE134 or SE131, Solarbio; 1:5000) at 37 °C for 45 min. Protein bands were visualized by the enhanced chemiluminescence system (PE0010, Solarbio) and quantified using Gel-Pro-Analyzer 4.0 (Media Cybernetics, USA). All primary antibodies used in this study have been verified for specificity by the manufacturer (Proteintech URL: https://www.ptgcn.com/;

Abclonal URL: https://abclonal.com.cn/; Santa cruz URL: https://www.scbt.com/customer-care/contact-us).

CCK-8 Assay

HRMECs were seeded into a 96-well plate overnight at a density of 3×10^3 cells per well and then maintained in control or HG medium for 48 h. Afterwards, 10 µl CCK-8 solution (96,992, Sigma) was added to each well and cultured at 37 °C for 1 h. The optical density (OD) value at 450 nm was detected using a microplate reader (800TS, BIOTEK, USA).

OIR Rat Model and Lentiviral Injection

All the procedures in animal experiments followed the Guide for the Care and Use of Laboratory Animals, and this study was approved by the Second Hospital of Jilin University. Pregnant Sprague–Dawley rats were purchased from ChangSheng Biotech. (China) and maintained at a temperature of 25 ± 1 °C, a humidity of 45–55% as well as a 12/12 h day-night cycle. The rats were allowed free access to water and food. Post natural delivery, neonatal rats were fed by maternal rats and divided into four groups ($n = 12$ pups /group) as follows: (1) sham; (2) OIR; (3) OIR + Control RNAi lentivirus (LV-shNC); and (4) OIR + LV-shKLF9. The model of OIR was established in rats by exposure to a 3-h 80–20% O_2 cycle daily from postnatal day (P) 0 until P11 [43]. Pups were then transferred into a normoxia environment and housed until P18 (retinal angiogenesis period). Sham rats were kept in a normoxia environment throughout the experiment. An hour after removing from the hyperoxia environment on P12, OIR pups were intravitreally injected with LV-shKLF9 or LV-shNC (1×10^8 TU/ml; 1 µl), or an equal volume of saline in the right eye [44]. On P18, all rats were anesthetized with pentobarbital sodium and their retinal tissues from right eyes were collected. In each group, retinal tissues collected from six pups were used for real-time (RT)-PCR analysis. Retinal tissues collected three pups were embedded into paraffin and cut into 5-µm slices for hematoxylin and eosin (H&E) staining and immunohistochemistry. Three slices from each retina were photographed at three random fields. The intact retinas from three pups were subjected to CD31 immunofluorescent assay. Representative images of morphological changes were shown in this study.

RT-PCR

Total RNA was extracted from retinal tissues and HRMECs using the RNAsimple Total RNA Kit (DP419, TIANGEN, China). The BeyoRT™ II M-MLV reverse transcriptase (D7160L, Beyotime, China) was used to obtain cDNA. The SYBR Green I (SY1020, Solarbio) was used for PCR amplification. The mRNA expression levels of KLF9 and YAP1 were evaluated using the $2^{-\Delta\Delta CT}$ method and β-actin was regarded as endogenous control. All primers were synthesized from GenScript (Nanjing, China) and their sequences were as follows: *homo* KLF9, forward 5′-TGGACCTGAACAAGTACCGA-3′, reverse 5′-TGTAATGGGCTTTGAGATGG-3′; *homo* YAP1, forward 5′-AAGGCTTGACCCTCGTTT-3′, reverse 5′-TTGCTGTGCTGGGATTGA-3′; *Rattus* KLF9, forward 5′-GTTGGACCTGAACAAATACCG-3′, reverse 5′-CCAGAGTGGAGGAGGGAGA-3′; *Rattus* VEGF, forward 5′-TCTTCAAGCCGTCCTGTG-3′, reverse 5′-CCTTTCCTCGAACTGATTTT-3′.

H&E Staining

Retinal tissues were fixed in 4% paraformaldehyde, embedded in paraffin, and cut into 5-µm sections. After deparaffinization and rehydration, sections were stained with H&E. These histological sections were examined under a light microscope (BX53, Olympus) at × 200 magnification.

Immunohistochemistry

Deparaffinized tissues were treated with citric acid buffer and 3% hydrogen peroxide. After blocking with goat serum for 15 min in the dark, tissues were incubated with anti-Ki67 (A2094, Abclonal; 1:100) primary antibody overnight at 4 °C, and then with horseradish peroxidase (HRP)-conjugated goat anti-rabbit IgG (#31,460, ThermoFisher, USA; 1:500) secondary antibody for 1 h at room temperature in the dark. Retinal tissues were analyzed with a microscope (BX53, Olympus) at × 400 magnification.

Immunofluorescence

Retinas embedded in paraffin were cut into 5-µm sections. After deparaffinization and rehydration, the slices were incubated in boiled citric acid buffer for 10 min, washed with PBS (1 ×) several times, and then blocked with goat serum for 15 min in dark at room temperature. For HRMECs, cells were fixed in 4% paraformaldehyde for 15 min, incubated in 0.1% TritonX-100 for 30 min, then washed with PBS (1 ×) to remove TritonX-100. Then, samples were incubated with anti-KLF9 (A7196, abclonal; 1:50), anti-Ki67 (A2094, Abclonal; 1:100) or anti-CD31 (AF6191, Affinity, China; 1:100) primary antibody overnight at 4 °C, followed by incubation with Cy3-tagged goat anti-rabbit IgG (A0516, Beyotime) secondary antibody for 1 h at room temperature in the dark. Afterwards, cells were counterstained with 4′,6-diamidino-2-phenylindole (DAPI) and mounted with an antifade mounting medium (Solarbio). Samples were photographed with a fluorescence microscope (BX53, Olympus) at × 400 magnification.

Statistical Analysis

Results were analyzed by GraphPad Prism 8.0 software. Values were shown as means ± standard deviation (SD). The one-way ANOVA (Tukey test) was used for comparisons of multiple groups. A $p < 0.05$ was considered significant.

Acknowledgements Not applicable.

Data Availability The data that support the findings of this study are available from the corresponding author upon reasonable request.

Declarations

Conflict of Interest The authors declare that they have no conflict of interest.

References

1. Cho, N. H., Shaw, J. E., Karuranga, S., Huang, Y., da Rocha Fernandes, J. D., Ohlrogge, A. W., & Malanda, B. (2018). IDF diabetes atlas: Global estimates of diabetes prevalence for 2017 and projections for 2045. *Diabetes Research and Clinical Practice, 138*, 271–281.
2. Stitt, A. W., Curtis, T. M., Chen, M., Medina, R. J., McKay, G. J., Jenkins, A., Gardiner, T. A., Lyons, T. J., Hammes, H. P., Simo, R., & Lois, N. (2016). The progress in understanding and treatment of diabetic retinopathy. *Progress in Retinal and Eye Research, 51*, 156–186.
3. Gucciardo, E., Loukovaara, S., Salven, P., & Lehti, K. (2018). Lymphatic vascular structures: a new aspect in proliferative diabetic retinopathy. *Int J Mol Sci., 19*, 4034.
4. Ruiz, M. A., Feng, B., & Chakrabarti, S. (2015). Polycomb repressive complex 2 regulates MiR-200b in retinal endothelial cells: Potential relevance in diabetic retinopathy. *PLoS ONE, 10*, e0123987.
5. Potente, M., Gerhardt, H., & Carmeliet, P. (2011). Basic and therapeutic aspects of angiogenesis. *Cell, 146*, 873–887.
6. Xu, Y., Lu, X., Hu, Y., Yang, B., Tsui, C. K., Yu, S., Lu, L., & Liang, X. (2018). Melatonin attenuated retinal neovascularization and neuroglial dysfunction by inhibition of HIF-1alpha-VEGF pathway in oxygen-induced retinopathy mice. *Journal of Pineal Research, 64*, e12473.
7. Bagati, A., Moparthy, S., Fink, E. E., Bianchi-Smiraglia, A., Yun, D. H., Kolesnikova, M., Udartseva, O. O., Wolff, D. W., Roll, M. V., Lipchick, B. C., Han, Z., Kozlova, N. I., Jowdy, P., Berman, A. E., Box, N. F., Rodriguez, C., Bshara, W., Kandel, E. S., Soengas, M. S., … Nikiforov, M. A. (2019). KLF9-dependent ROS regulate melanoma progression in stage-specific manner. *Oncogene, 38*, 3585–3597.
8. Tetreault, M. P., Yang, Y., & Katz, J. P. (2013). Kruppel-like factors in cancer. *Nature Reviews Cancer, 13*, 701–713.
9. He, X., & Zeng, X. (2020). LncRNA SNHG16 aggravates high glucose-induced podocytes injury in diabetic nephropathy through targeting miR-106a and thereby up-regulating KLF9. *Diabetes, Metabolism, Syndrome and Obesity: Targets and Therapy, 13*, 3551–3560.
10. Cui, A., Fan, H., Zhang, Y., Zhang, Y., Niu, D., Liu, S., Liu, Q., Ma, W., Shen, Z., Shen, L., Liu, Y., Zhang, H., Xue, Y., Cui, Y., Wang, Q., Xiao, X., Fang, F., Yang, J., Cui, Q., & Chang, Y. (2019). Dexamethasone-induced Kruppel-like factor 9 expression promotes hepatic gluconeogenesis and hyperglycemia. *The Journal of Clinical Investigation, 129*, 2266–2278.
11. Li, H., Weng, Y., Lai, L., Lei, H., Xu, S., Zhang, Y., & Li, L. (2021). KLF9 regulates PRDX6 expression in hyperglycemia-aggravated bupivacaine neurotoxicity. *Molecular and Cellular Biochemistry, 476*, 2125–2134.
12. Ma, L., Li, Z., Li, W., Ai, J., & Chen, X. (2019). MicroRNA-142-3p suppresses endometriosis by regulating KLF9-mediated autophagy in vitro and in vivo. *RNA Biology, 16*, 1733–1748.
13. Piccolo, S., Dupont, S., & Cordenonsi, M. (2014). The biology of YAP/TAZ: Hippo signaling and beyond. *Physiological Reviews, 94*, 1287–1312.
14. Wen, D., Wang, L., Tan, S., Tang, R., Xie, W., Liu, S., Tang, C., & He, Y. (2020). HOXD9 aggravates the development of cervical cancer by transcriptionally activating HMCN1. *Panminerva Medica*. https://doi.org/10.23736/S0031-0808.20.03911-7
15. Chen, J., Wang, X., He, Q., Bulus, N., Fogo, A. B., Zhang, M. Z., & Harris, R. C. (2020). YAP activation in renal proximal tubule cells drives diabetic renal interstitial fibrogenesis. *Diabetes, 69*, 2446–2457.
16. Liu, J., Xu, L., & Zhan, X. (2020). LncRNA MALAT1 regulates diabetic cardiac fibroblasts through the Hippo-YAP signaling pathway. *Biochemistry and Cell Biology, 98*, 537–547.
17. Pan, Q., Gao, Z., Zhu, C., Peng, Z., Song, M., & Li, L. (2020). Overexpression of histone deacetylase SIRT1 exerts an antiangiogenic role in diabetic retinopathy via miR-20a elevation and YAP/HIF1alpha/VEGFA depletion. *American Journal of Physiology: Endocrinology and Metabolism, 319*, E932–E943.
18. Han, N., Tian, W., Yu, N., & Yu, L. (2020). YAP1 is required for the angiogenesis in retinal microvascular endothelial cells via the inhibition of MALAT1-mediated miR-200b-3p in high glucose-induced diabetic retinopathy. *Journal of Cellular Physiology, 235*, 1309–1320.
19. Wang, Z., Xing, W., Song, Y., Li, H., Liu, Y., Wang, Y., Li, C., Wang, Y., Wu, Y., & Han, J. (2018). Folic acid has a protective effect on retinal vascular endothelial cells against high glucose. *Molecules., 23*, 2326.
20. Lam, J. D., Oh, D. J., Wong, L. L., Amarnani, D., Park-Windhol, C., Sanchez, A. V., Cardona-Velez, J., McGuone, D., Stemmer-Rachamimov, A. O., Eliott, D., Bielenberg, D. R., van Zyl, T., Shen, L., Gai, X., D'Amore, P. A., Kim, L. A., & Arboleda-Velasquez, J. F. (2017). Identification of RUNX1 as a mediator of aberrant retinal angiogenesis. *Diabetes, 66*, 1950–1956.
21. Connor, K. M., Krah, N. M., Dennison, R. J., Aderman, C. M., Chen, J., Guerin, K. I., Sapieha, P., Stahl, A., Willett, K. L., & Smith, L. E. (2009). Quantification of oxygen-induced retinopathy in the mouse: A model of vessel loss, vessel regrowth and pathological angiogenesis. *Nature Protocols, 4*, 1565–1573.
22. Fernando, K. H. N., Yang, H. W., Jiang, Y., Jeon, Y. J., & Ryu, B. (2018). Diphlorethohydroxycarmalol isolated from Ishige okamurae represses high glucose-induced angiogenesis in vitro and in vivo. *Mar Drugs., 16*, 375.
23. Li, R., Du, J., Yao, Y., Yao, G., & Wang, X. (2019). Adiponectin inhibits high glucose-induced angiogenesis via inhibiting autophagy in RF/6A cells. *Journal of Cellular Physiology, 234*, 20566–20576.
24. Wang, Y., Wang, L., Guo, H., Peng, Y., Nie, D., Mo, J., & Ye, L. (2020). Knockdown of MALAT1 attenuates high-glucose-induced angiogenesis and inflammation via endoplasmic reticulum stress in human retinal vascular endothelial cells. *Biomedicine & Pharmacotherapy, 124*, 109699.
25. Fallah, A., Sadeghinia, A., Kahroba, H., Samadi, A., Heidari, H. R., Bradaran, B., Zeinali, S., & Molavi, O. (2019). Therapeutic targeting of angiogenesis molecular pathways in

angiogenesis-dependent diseases. *Biomedicine & Pharmacotherapy, 110*, 775–785.
26. Hartnett, M. E. (2015). Pathophysiology and mechanisms of severe retinopathy of prematurity. *Ophthalmology, 122*, 200–210.
27. Abdullah, S. E., & Perez-Soler, R. (2012). Mechanisms of resistance to vascular endothelial growth factor blockade. *Cancer, 118*, 3455–3467.
28. Lee, J. W., Ko, J., Ju, C., & Eltzschig, H. K. (2019). Hypoxia signaling in human diseases and therapeutic targets. *Experimental & Molecular Medicine, 51*, 1–13.
29. Han, N., Xu, H., Yu, N., Wu, Y., & Yu, L. (2020). MiR-203a-3p inhibits retinal angiogenesis and alleviates proliferative diabetic retinopathy in oxygen-induced retinopathy (OIR) rat model via targeting VEGFA and HIF-1alpha. *Clinical and Experimental Pharmacology and Physiology, 47*, 85–94.
30. Zhang, W. Y., Wang, J., & Li, A. Z. (2020). A study of the effects of SGLT-2 inhibitors on diabetic cardiomyopathy through miR-30d/KLF9/VEGFA pathway. *European Review for Medical and Pharmacological Sciences, 24*, 6346–6359.
31. Millimaggi, D., Mari, M., D'Ascenzo, S., Carosa, E., Jannini, E. A., Zucker, S., Carta, G., Pavan, A., & Dolo, V. (2007). Tumor vesicle-associated CD147 modulates the angiogenic capability of endothelial cells. *Neoplasia, 9*, 349–357.
32. Abu El-Asrar, A. M., Ahmad, A., Alam, K., Siddiquei, M. M., Mohammad, G., Hertogh, G., Mousa, A., & Opdenakker, G. (2017). Extracellular matrix metalloproteinase inducer (EMMPRIN) is a potential biomarker of angiogenesis in proliferative diabetic retinopathy. *Acta Ophthalmologica, 95*, 697–704.
33. Noda, K., Ishida, S., Inoue, M., Obata, K., Oguchi, Y., Okada, Y., & Ikeda, E. (2003). Production and activation of matrix metalloproteinase-2 in proliferative diabetic retinopathy. *Investigative Ophthalmology & Visual Science, 44*, 2163–2170.
34. Zhong, Z., Zhou, F., Wang, D., Wu, M., Zhou, W., Zou, Y., Li, J., Wu, L., & Yin, X. (2018). Expression of KLF9 in pancreatic cancer and its effects on the invasion, migration, apoptosis, cell cycle distribution, and proliferation of pancreatic cancer cell lines. *Oncology Reports, 40*, 3852–3860.
35. Zhu, M., Liu, X., Wang, Y., Chen, L., Wang, L., Qin, X., Xu, J., Li, L., Tu, Y., Zhou, T., Sang, A., & Song, E. (2018). YAP via interacting with STAT3 regulates VEGF-induced angiogenesis in human retinal microvascular endothelial cells. *Experimental Cell Research, 373*, 155–163.
36. Yan, Z., Shi, H., Zhu, R., Li, L., Qin, B., Kang, L., Chen, H., & Guan, H. (2018). Inhibition of YAP ameliorates choroidal neovascularization via inhibiting endothelial cell proliferation. *Molecular Vision, 24*, 83–93.
37. Potilinski, M. C., Lorenc, V., Perisset, S., & Gallo, J. E. (2020). Mechanisms behind retinal ganglion cell loss in diabetes and therapeutic approach. *International Journal of Molecular Sciences, 21*, 2351.
38. Amato, R., Lazzara, F., Chou, T. H., Romano, G. L., Cammalleri, M., Dal Monte, M., Casini, G., & Porciatti, V. (2021). Diabetes exacerbates the intraocular pressure-independent retinal ganglion cells degeneration in the DBA/2J model of glaucoma. *Investigative Ophthalmology & Visual Science, 62*, 9.
39. Apara, A., Galvao, J., Wang, Y., Blackmore, M., Trillo, A., Iwao, K., Brown, D. P., Jr., Fernandes, K. A., Huang, A., Nguyen, T., Ashouri, M., Zhang, X., Shaw, P. X., Kunzevitzky, N. J., Moore, D. L., Libby, R. T., & Goldberg, J. L. (2017). KLF9 and JNK3 interact to suppress axon regeneration in the adult CNS. *Journal of Neuroscience, 37*, 9632–9644.
40. Galvao, J., Iwao, K., Apara, A., Wang, Y., Ashouri, M., Shah, T. N., Blackmore, M., Kunzevitzky, N. J., Moore, D. L., & Goldberg, J. L. (2018). The Kruppel-like factor gene target dusp14 regulates axon growth and regeneration. *Investigative Ophthalmology & Visual Science, 59*, 2736–2747.
41. Xie, J., Gong, Q., Liu, X., Liu, Z., Tian, R., Cheng, Y., & Su, G. (2017). Transcription factor SP1 mediates hyperglycemia-induced upregulation of roundabout4 in retinal microvascular endothelial cells. *Gene, 616*, 31–40.
42. Cao, X., Xue, L. D., Di, Y., Li, T., Tian, Y. J., & Song, Y. (2021). MSC-derived exosomal lncRNA SNHG7 suppresses endothelial-mesenchymal transition and tube formation in diabetic retinopathy via miR-34a-5p/XBP1 axis. *Life Sciences, 272*, 119232.
43. Wilkinson-Berka, J. L., Tan, G., Jaworski, K., Harbig, J., & Miller, A. G. (2009). Identification of a retinal aldosterone system and the protective effects of mineralocorticoid receptor antagonism on retinal vascular pathology. *Circulation Research, 104*, 124–133.
44. Deliyanti, D., Zhang, Y., Khong, F., Berka, D. R., Stapleton, D. I., Kelly, D. J., & Wilkinson-Berka, J. L. (2015). FT011, a novel cardiorenal protective drug, reduces inflammation, gliosis and vascular injury in rats with diabetic retinopathy. *PLoS ONE, 10*, e0134392.